

Constrained Bithiazoles: Small Molecule Correctors of Defective $\Delta F508$ –CFTR Protein Trafficking

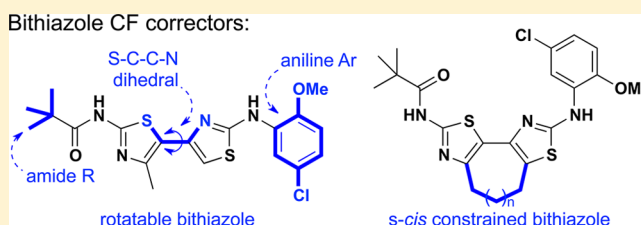
Keith C. Coffman,[†] Huy H. Nguyen,[†] Puay-Wah Phuan,[‡] Brandi M. Hudson,[†] Gui J. Yu,[†] Alex L. Bagdasarjan,[†] Deanna Montgomery,[†] Michael W. Lodewyk,[†] Baoxue Yang,[‡] Choong L. Yoo,[†] A. S. Verkman,[‡] Dean J. Tantillo,[†] and Mark J. Kurth^{*,†}

[†]Department of Chemistry, University of California, One Shields Avenue, Davis, California 95616, United States

[‡]Department of Medicine and Physiology, University of California, 513 Parnassus Avenue, San Francisco, California 94143, United States

S Supporting Information

ABSTRACT: Conformationally constrained bithiazoles were previously found to have improved efficacy over nonconstrained bithiazoles for correction of defective cellular processing of the $\Delta F508$ mutant cystic fibrosis transmembrane conductance regulator (CFTR) protein. In this study, two sets of constrained bithiazoles were designed, synthesized, and tested in vitro using $\Delta F508$ –CFTR expressing epithelial cells. The SAR data demonstrated that modulating the constraining ring size between 7- versus 8-membered in these constrained bithiazole correctors did not significantly enhance their potency (IC_{50}), but strongly affected maximum efficacy (V_{max}), with constrained bithiazoles **9e** and **10c** increasing V_{max} by 1.5-fold compared to benchmark bithiazole **corr4a**. The data suggest that the 7- and 8-membered constrained ring bithiazoles are similar in their ability to accommodate the requisite geometric constraints during protein binding.



INTRODUCTION

Cystic fibrosis (CF) is a recessive genetic disease found primarily in Caucasians.¹ Of the ~2000 known mutations in the CF gene, deletion of phenylalanine at position 508 ($\Delta F508$) in the cystic fibrosis transmembrane conductance regulator (CFTR) protein is the most common mutation, present in at least one allele in ~90% of patients.^{2–4} Due to this deletion, the $\Delta F508$ –CFTR protein is misfolded, retained at the endoplasmic reticulum, and rapidly degraded.⁴ CFTR protein is a cyclic AMP-regulated chloride channel expressed in the plasma membrane of secretory epithelia in the airways, intestines, pancreas, testes, and exocrine glands, as well as some nonepithelial cell types.^{4,5} CF patients suffer from chronic lung infections leading to deterioration of lung function, which is the main cause of morbidity and mortality.⁴ Currently, there is only one drug (potentiator) that targets mutant CFTR (KalydecoTM; VX-770), but it is only helpful to the small number of patients with the G551D mutation (4.3% of CF patients) and some other gating mutations.^{3,6}

Correctors, first recognized by Verkman et al.,^{5a} are believed to address the misfolding and trafficking of defective $\Delta F508$ –CFTR protein and are being investigated by several groups.⁶ The investigational correctors VX-809 and VX-661 are in clinical trials.⁷ However, the limited understanding of how small molecules modulate the trafficking of $\Delta F508$ –CFTR creates a challenge in efforts to discover effective corrector drug candidates. We previously reported that bithiazoles (cf., **corr4a** and **corr15jf**, Figure 1) can correct $\Delta F508$ –CFTR, and these

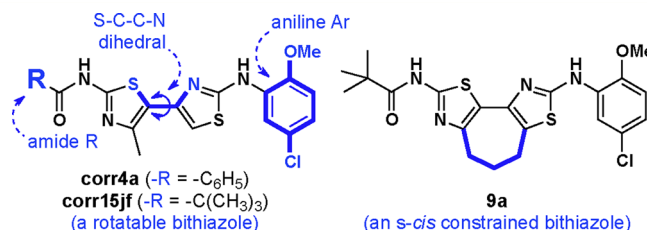


Figure 1. Constrained bithiazole corrector **9a**, lead corrector **corr15jf**, and benchmark corrector **corr4a**.

studies showed that the conformation of the bithiazole core structure is an important determinant of corrector activity. Corrector **9a** (Figure 1), with its constrained bithiazole substructure compared to lead bithiazole **corr15jf**, was identified in these previous studies.⁸

The present study was designed to explore the constrained bithiazole core further by (1) defining the optimum size of the ring constraining the bithiazole core and (2) refining the peripheral groups in these constrained correctors using in vitro evaluation with $\Delta F508$ –CFTR FRT epithelial cells. It is hoped that refined bithiazole structural features may lead to useful insight into the mechanism of small molecule $\Delta F508$ –CFTR protein binding and interactions.^{8,9}

Received: May 20, 2014

Published: July 16, 2014



Constrained bithiazoles are of particular interest because the bithiazole moiety is found in some natural products.¹⁰ Also, bithiazole **9a**, with its constrained conformational advantage over freely rotating bithiazoles **corr4a** and **corr15jf**, can be expected to have a more favorable entropy of binding in formation of the corrector-bound-CFTR complex.¹¹ Herein, we report the synthesis and biological evaluation of a set of novel constrained bithiazoles.

CHEMISTRY

On the basis of our previous bithiazole studies,^{8,12} we were interested in exploring different constraining ring sizes in the bithiazole core substructure. Indeed, as the ring size increases or decreases, the bithiazole substructure becomes more or less rigid, and the interatomic distances and dihedral angles between the thiazole rings modulate. To fully probe these structural features, the constraining carbocycle (red highlight in **1**; Figure 2) would, ideally, range from five to eight-membered rings (i.e., $m = 0-3$ in generalized bithiazole **1**).

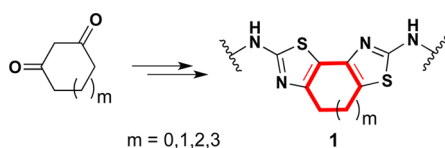


Figure 2. Target analogues (**1**) of constrained bithiazole corrector **9a**.

For $1^m = 0$ (5-membered constrained bithiazole **2**; Figure 3), a variety of routes were explored without success. For instance, α -

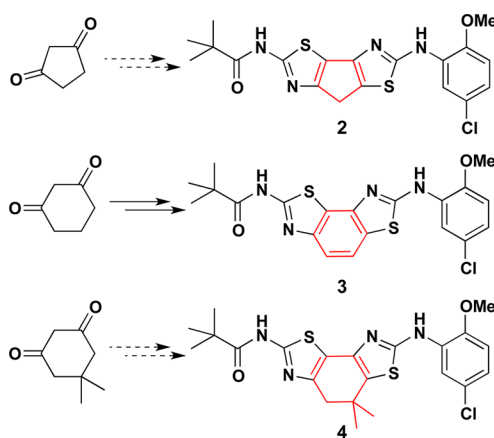


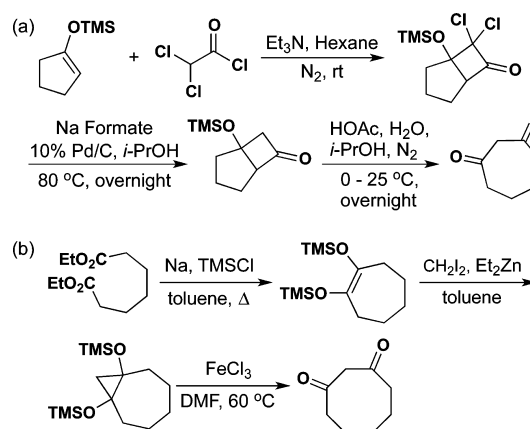
Figure 3. Constrained bithiazole analogues **2-4**.

bromination of 1,3-cyclopentanedione followed by displacement with thiourea cleanly gave 2-amino-4H-cyclopenta[d]-thiazol-6(5H)-one. The introduction of the second thiazole ring by a second α -bromination and subsequent condensation with a substituted thiourea failed, even at elevated temperatures in a microwave reactor, to give the targeted bithiazole **2**. Presumably the 5,5,5-ring system in **2** is too strained to form under these conditions. In contrast, the first and second thiazole-forming steps for $1^m = 1$ (6-membered constraining ring) proceeded smoothly, but during the final *N*-acylation step, the central cyclohexadiene ring spontaneously aromatized (even at -4°C) to give **3** (Figure 3). To avoid this aromatization, we employed 5,5-dimethyl-1,3-cyclohexanedione and found that the first bromination/thiazole formation sequence worked well. However, as with 1,3-cyclopentane-

dione, the second bromination/thiazole formation sequence failed to deliver the targeted bithiazole because S_N2 reaction on the neopentyl bromide failed under all conditions attempted (for example, using AgBF_6 to activate the C–Br bond). Consequently, the only constrained bithiazole $1^m = 1$ evaluated in vitro (vide supra) was aromatized analogue **3**.

We next directed our attention to the preparation of constrained bithiazoles **9** ($1^m = 2$; 7-membered constraining ring) and **10** ($1^m = 3$; 8-membered constraining ring). This series contained constrained corrector **9a** plus several amide (e.g., “R” in **9a-f/10a-f**; Scheme 2a) and aniline (e.g., “Ar” in **9g-j/10g-j**; Scheme 2b) analogues. These various constrained bithiazoles were synthesized by modification of our previously published procedures^{8,12} starting from 1,3-cycloheptadione [prepared from (cyclopent-1-en-1-yloxy)trimethylsilane as outlined in Scheme 1a]⁸ and 1,3-cyclooctadione (prepared from diethyl heptanedioate as outlined in Scheme 1b).¹³

Scheme 1. (a) Synthesis of 1,3-Cycloheptadione. (b) Synthesis of 1,3-Cyclooctadione



With the requisite diones in hand, α -bromination [$\text{CHCl}_3/\text{H}_2\text{O}$ (1:1) for 1,3-cycloheptadione; $\text{CCl}_4/\text{H}_2\text{O}$ (1:1) for 1,3-cyclooctadione] by the dropwise addition of bromine at 0°C followed by treatment of the crude 2-bromo-1,3-dione with thiourea in ethanol overnight delivered thiazoles **5** and **6** in 38% and 51% yield, respectively, over two steps. As a result of the difficulty in workup, thiazole **6** required basification (sat. NH_4OH to pH 8–9) before purification followed by reacidification (HBr in HOAc) ahead of the second bromination. Following a second α -bromination by dropwise addition of bromine to **5** or **6** in HOAc, the resulting α -bromoketone was refluxed in EtOH overnight with 1-(5-chloro-2-methoxyphenyl)thiourea to yield **7a** and **8a** in 79% and 65% yield, respectively. Bithiazoles **7a** and **8a** were stirred in DCM and Et_3N at 60°C overnight with various acid chlorides to give the final constrained bithiazoles **9a-f** and **10a-f**. Constrained bithiazoles **9g-j** and **10g-j**, wherein the amide moiety was maintained as a pivalamide and the aniline aryl moiety was varied, were prepared in similar fashion, except that different aryl substituted thioureas were used to prepare **7g-j** and **8g-j**.

ΔF508 –CFTR CORRECTION BIOASSAY

The screening assay utilized Fischer rat thyroid (FRT) epithelial cells coexpressing ΔF508 –CFTR and the yellow fluorescent protein (YFP) halide indicator YFP-H148Q/I152L at 37°C in a 96-well-plate format.^{5,8,12} Correctors at various

concentrations (and negative/positive controls) were added to each well and incubated for 18–24 h. $\Delta F508$ –CFTR-facilitated iodide influx was determined from the kinetics of YFP-H148Q/I152L quenching in response to iodide addition in cells treated with a cAMP agonist forskolin and the potentiator genistein.

RESULTS AND DISCUSSION

Prior bithiazole-based structure–activity relationship studies supported the premise that the conformation about the bithiazole moiety is an important determinant of $\Delta F508$ –CFTR corrector activity.⁸ Although bithiazoles that are free to rotate around the thiazole–thiazole tethering C,C-bond can accommodate many conformations, we went on to demonstrate that constrained bithiazoles—where the bithiazole moiety was locked into an *s-cis* conformation (see Figure 1)—led to improved corrector activity.⁸ With this backdrop, the objectives of this investigation were 3-fold: (i) correlate corrector activity with bithiazole S–C–C–N (see **corr4a** in Figure 1) dihedral angle; (ii) correlate corrector activity with amide R-group (see **corr4a** in Figure 1) structural features; and (iii) correlate corrector activity with aniline Ar (see **corr4a** in Figure 1) structural features.

Our inability to construct the 7*H*-cyclopenta[1,2-*d*:3,4-*d'*]bis(thiazole) analogue of **1** (*m* = 0) coupled with the fact that the 4,5-dihydrobenzo[1,2-*d*:3,4-*d'*]bis(thiazole) analogue of **1** (*m* = 1) spontaneously aromatizes to **3** limited the probe of lower value S–C–C–N dihedral angle to 0°. Moreover, fully aromatized bithiazole **3** proved to be toxic, killing the $\Delta F508$ –CFTR transfected FRT cells employed in the assay. These outcomes evolved objective (i) of this study to a direct comparison of constrained bithiazoles **9a** (*m* = 2) and **10a** (*m* = 3) to benchmark bithiazole corrector **corr4a** (these three correctors each has the aniline Ar = 5-chloro-2-methoxyphenyl). The IC_{50} values of **9a** and **10a** (2.3 and 4.1 μM , respectively) were improved relative to **corr4a** (6.0 μM), and the 8-membered constrained corrector **10a** was found to have a higher V_{max} value (Table 1; 512 $\mu M/s$) than either the 7-membered analogue **9a** (Table 1; 336 $\mu M/s$) or **corr4a** (V_{max} = 475 $\mu M/s$).

With comparable IC_{50} values for **9a**, **10a**, and **corr4a** and a higher V_{max} value for **10a**, we were encouraged to continue the exploration of these 7- and 8-membered constrained bithiazole analogues. On the basis of previous research into the bithiazole class of compounds,^{8,12} we knew that the amide moiety of the bithiazole had improved activity as a pivalamide group compared to a benzamide. A series of six pivalamide-like constrained bithiazoles (Scheme 2a; **9b–e** and **10b–e**) as well as four pivalamide-unlike constrained bithiazoles (Scheme 2a; ethyl propanoates **9e/10e** and isoxazoles **9f/10f**)—all with 5-chloro-2-methoxyphenyl as the aniline moiety—were prepared and evaluated for $\Delta F508$ –CFTR corrector activity. Although the IC_{50} values for this set of amides did not reveal any significant increase or decrease in activity relative to **corr4a**, there were significantly improved V_{max} values for **9e** (678 $\mu M/s$) and **10c** (717 $\mu M/s$) relative to **corr4a** (475 $\mu M/s$). Importantly, these increases in V_{max} are indicative of better chloride cell permeability in the rescued $\Delta F508$ –CFTR protein. Finally, although their IC_{50} values were highest in the Table 1 series, we were surprised to find that free amine analogues **7a** and **8a** were modest correctors with V_{max} values approximately similar to amides **9a–f** and **10a–f**.

Our next objective was to explore modification of the aniline aryl moiety in these constrained bithiazoles. Previous SAR

Table 1. Corrector Activities of Amide-Varied Constrained Bithiazoles 7a/8a and 9a–f/10a–f Relative to Bithiazole corr4a

corr4a: ^a V_{max} = 475 $\mu M/s$, IC_{50} = 6.0 μM					
compound	9a–f; <i>n</i> = 1		compound	10a–f; <i>n</i> = 2	
	V_{max} ($\mu M/s$)	IC_{50} (μM)		V_{max} ($\mu M/s$)	IC_{50} (μM)
7a	351	11.0	8a	592	9.2
9a	336	2.3	10a	512	4.1
9b	473	8.9	10b	247	4.5
9c	329	5.8	10c	717	8.7
9d	447	6.6	10d	286	2.9
9e	678	8.8	10e	481	8.3
9f	505	4.8	10f	467	6.6

^aCorrector activity of benchmark bithiazole **corr4a**.

data^{8,12} suggested that the electron-withdrawing groups (EWG) on the phenyl ring, like fluorine, reduce corrector activity, whereas electron-donating groups (EDG) on the phenyl ring, like methoxy, improve corrector activity. However, we noted that the aryls substituted simultaneously with EWG and EDG like -Cl and -OMe generally were among the better correctors. Also, LogP is an important feature in drug design, and we reasoned that *N*-alkylated aniline or pyridine moieties could form ammonium salts to facilitate hydrophilicity. Therefore, we set out to prepare constrained bithiazole analogues **9a,g–j** and **10a,g–j** to probe these two issues. As outlined in Table 2, all of

Table 2. Corrector Activities of Aniline-Varied Constrained Bithiazoles 9a/10a and 9g–j/10g–j Relative to Bithiazole corr4a

corr4a: ^a V_{max} = 475 $\mu M/s$, IC_{50} = 6.0 μM					
compound	9a,g–j <i>n</i> = 1		compound	10a,g–j <i>n</i> = 2	
	V_{max} ($\mu M/s$)	IC_{50} (μM)		V_{max} ($\mu M/s$)	IC_{50} (μM)
9a	336	2.3	10a	512	4.1
9g	366	6.9	10g	198	2.1
9h	509	7.2	10h	280	5.2
9i	336	2.2	10i	291	5.2
9j	485	3.6	10j	243	0.9

^aCorrector activity of benchmark bithiazole **corr4a**.

the constrained bithiazoles in this series were active correctors. Of the set, 7-membered bithiazole **9i** and 8-membered bithiazoles **10g** and **10j** had the lowest IC_{50} values. Only 7-membered constrained bithiazoles **9h** and **9j** afforded a significant V_{max} improvement relative to **9a**.

In an effort to understand the relationship between ring size and activity, a search of possible conformations of each of the bithiazole analogues (including full optimizations with density functional theory) was carried out. Figure 4 shows the two lowest energy conformations of bithiazoles **3**, **9a**, and **10a**. Not surprisingly, more conformations of **9a** and **10a** are accessible compared to **3**. Constrained bithiazoles **9a** and **10a** are not forced into a flat U-shaped conformation (i.e., a central dihedral angle of 0°), which is perhaps related to the cytotoxicity of **3** (although this may also be a result of increased unsaturation). Because the size of the fused ring (7-membered vs 8-membered) does not significantly affect activity, it seems that

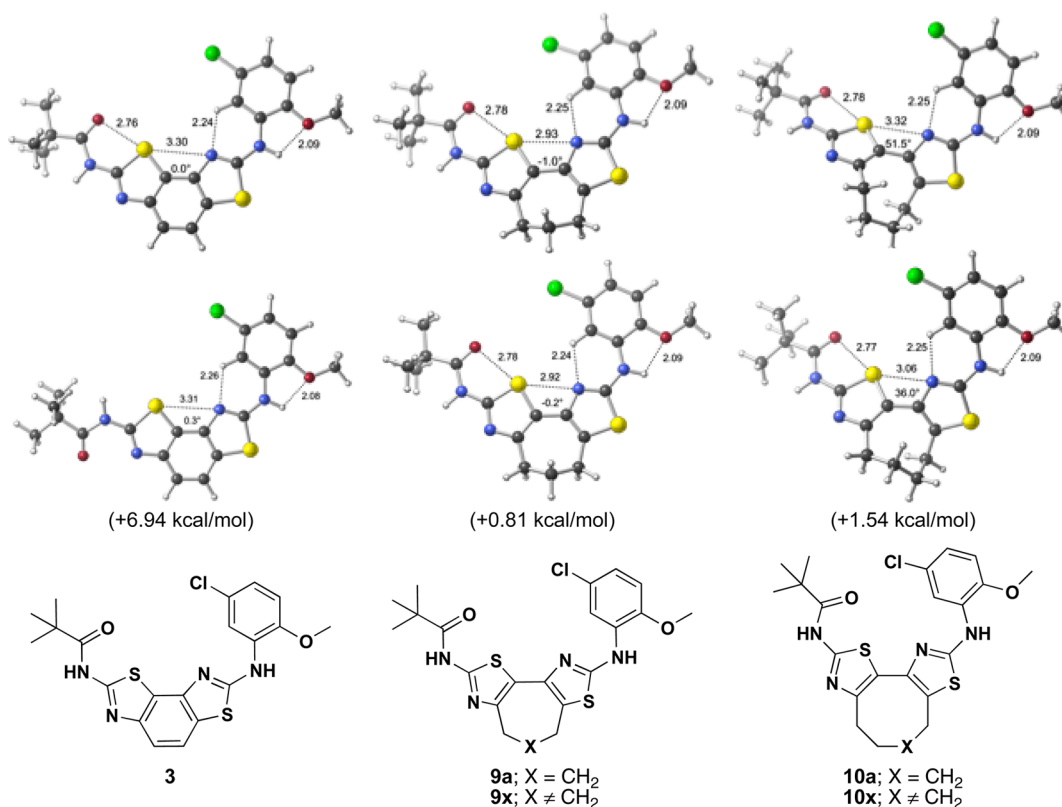


Figure 4. Lowest energy conformers of 3, 9a, and 10a. Geometries and energies were computed with M06-2X/6-31+G(d,p) (selected distances are shown in Å; dihedral angles are shown for the central S–C–C–N substructure; see the Computational Methods section in Supporting Information for values and details). Top structures are the lowest energy conformers, whereas bottom structures are the second lowest energy conformers; free energies for the latter relative to the former (0.0 kcal/mol) are shown in kcal/mol.

the target active site can accommodate nonpolar moieties of varying size and shape.

On the basis of these structural insights, future discovery on constrained bithiazoles could address how structural manipulation of the 7- and 8-membered constraining ring might improve compound potency, pharmacokinetics, and pharmacodynamics. Two broadly cast “constrained-X” options (9x and 10x) are depicted in Figure 4. Although 7-membered analogue 9x is appealing from a symmetry perspective, Scheme 2 chemistry may be complicated by regiochemical issues imposed by the nonsymmetrical starting 1,3-dicarbonyl. The 8-membered analogue 10x, which could be prepared from a symmetrical 1,3-dicarbonyl starting material, would avoid these complications. Finally, in addition to various constrained-X modifications, manipulation of the peripheral groups (i.e., the amide “R” and aniline “Ar” moieties; see Scheme 2) in constrained-X analogues 9x and 10x may prove insightful.

CONCLUSIONS

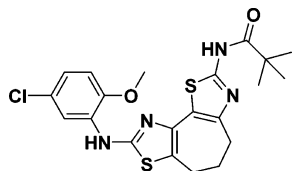
Twenty-three analogues of constrained bithiazole 9a were designed and synthesized to probe how the constrained bithiazole core affects the rescue and chloride channel function of Δ F508–CFTR. We found that modulating the constraining ring size (7- vs 8-membered) in these constrained bithiazole correctors did not significantly increase or decrease the potency (IC₅₀). However, the cell chloride permeability (V_{\max}) of corrected Δ F508–CFTR was significantly influenced by bithiazole peripheral groups; most notably, bithiazoles 9e and 10c had V_{\max} 200 μ M/s higher than benchmark bithiazole corr4a while maintaining comparable IC₅₀ values. This suggests

that the 7- and 8-membered ring sizes studied accommodate the requisite flexibility in the bithiazole core during protein binding.

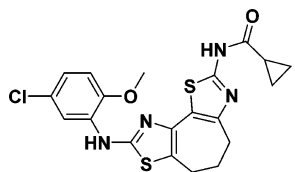
EXPERIMENTAL SECTION

General Procedures. All chemicals were purchased from commercial suppliers and used without further purification. Analytical thin layer chromatography was carried out on precoated plates (silica gel 60 F254, 250 μ m thickness) and visualized with UV light. Flash chromatography was performed using 60 Å, 32–63 μ m silica gel (Scientific Adsorbents). Concentration in vacuo refers to rotary evaporation under reduced pressure. The chemical purity of all compounds was determined by HPLC and HRMS or LC–MS and confirmed to be $\geq 95\%$. ¹H NMR spectra were recorded at 300, 400, 600, or 800 MHz at ambient temperature with acetone-*d*₆, DMSO-*d*₆, CDCl₃, CD₃CN, or CD₃OD as solvents. ¹³C NMR spectra were recorded at 75, 100, 150, or 200 MHz at ambient temperature with acetone-*d*₆, DMSO-*d*₆, CDCl₃, CD₃CN, or D₂O as solvents. Chemical shifts are reported in parts per million (ppm) relative to the residual solvent peak. Infrared spectra were recorded on an ATI-FTIR spectrometer. The specifications of the Waters LC/MS are as follows: electrospray (+) ionization, mass range 100–1500 Da, 20 V cone voltage, and Xterra MS C18 column (2.1 mm \times 50 mm \times 3.5 μ m), 0.2 mL/min; eluents were water/0.1% HCOOH and MeCN/0.1% HCOOH in gradient, and Waters 996 PDA. Preparative HPLC specifications are as follows: 15 mL/min flow rate, Xterra Prep MS C18 OBD column (19 mm \times 100 mm); eluents were water/0.1% HCOOH and MeCN/0.1% HCOOH in gradient, and dual wavelength absorbance detector. High-resolution mass spectra were acquired on an LTQ Orbitrap XL mass spectrometer equipped with an electrospray ionization source (ThermoFisher, San Jose, CA), operating in the positive ion mode. Samples were introduced into the source via loop injection at a flow rate of 200 μ L/min, in a solvent

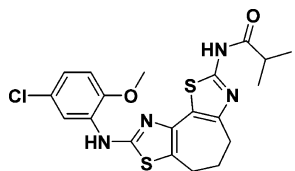
8.07 (d, $J = 2.4$ Hz, 1H), 7.57 (s, 1H), 6.92 (dd, 2.4 and 8.4 Hz, 1H), 6.78 (d, $J = 8.4$ Hz, 1H), 3.90 (s, 3H), 3.06 (at, 5.7 Hz, 2H), 2.98 (at, 5.6 Hz, 2H), 2.17–2.13 (m, 2H), 1.34 (s, 9H). ^{13}C NMR (150 MHz, CDCl_3): δ 184.2, 176.2, 158.9, 157.0, 145.5, 145.0, 138.6, 130.8, 126.3, 120.8, 120.1, 115.9, 110.6, 56.0, 39.2, 32.0, 27.2, 27.1, 22.6. HRMS (m/z): $[\text{M} + \text{H}]^+$ calcd for $\text{C}_{21}\text{H}_{23}\text{ClN}_4\text{O}_2\text{S}_2$, 463.1024; found, 463.1021.



N-(8-((5-Chloro-2-methoxyphenyl)amino)-5,6-dihydro-4H-cyclohepta[1,2-d:3,4-d']bis(thiazole)-2-yl)-cyclopropanecarboxamide (9b). The procedure for **9a** was followed, except cyclopropanecarboxamide (0.14 mmol, 2.6 equiv) (prepared freshly from cyclopropane carboxylic acid and oxalyl chloride 1:1.2 eq in 50 μL of DCM and a drop of DMF) was substituted, yielding a yellow solid (12 mg, 51%). ^1H NMR (600 MHz, CDCl_3): δ 8.05 (d, $J = 2.3$ Hz, 1H), 7.57 (s, 1H), 6.91 (dd, $J = 8.6$, 2.3 Hz, 1H), 6.77 (d, $J = 8.6$, 1H), 3.89 (s, 3H), 3.09 (at, $J = 5.5$ Hz, 2H), 2.98 (at, $J = 5.5$ Hz, 2H), 2.16–2.12 (m, 2H), 1.70–1.64 (m, 1H), 1.23–1.20 (m, 2H), 0.98–0.95 (m, 2H). ^{13}C NMR (150 MHz, CDCl_3): δ 171.4, 159.1, 156.8, 145.6, 143.5, 138.1, 130.7, 126.3, 122.7, 120.9, 120.6, 116.0, 110.7, 56.0, 31.9, 29.7, 27.0, 22.4, 15.1, 9.3. HRMS (m/z): $[\text{M} + \text{H}]^+$ calcd for $\text{C}_{20}\text{H}_{19}\text{ClN}_4\text{O}_2\text{S}_2$, 447.0711; found, 447.0708.

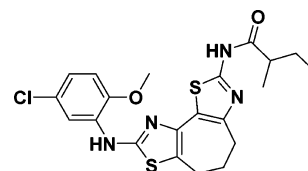


N-(8-((5-Chloro-2-methoxyphenyl)amino)-5,6-dihydro-4H-cyclohepta[1,2-d:3,4-d']bis(thiazole)-2-yl)isobutyramide (9c). The procedure for **9a** was followed, except isobutyryl chloride (7.2 μL , 0.069 mmol, 1.3 equiv) was substituted, yielding an orange solid (5.9 mg, 25%). mp 208–215 $^\circ\text{C}$. IR (neat): ν_{max} 2964, 2924, 1597, 1531, 1417, 1268, 1248, 1126, 1026, 796 cm^{-1} . ^1H NMR (600 MHz, CDCl_3): δ 8.21 (s, 1H), 8.06 (d, $J = 2.5$ Hz, 1H), 7.59 (s, 1H), 6.92 (dd, $J = 8.6$, 2.5 Hz, 1H), 6.78 (d, $J = 8.6$ Hz, 1H), 3.90 (s, 3H), 3.04 (at, $J = 5.7$ Hz, 2H), 2.98 (at, $J = 5.6$ Hz, 2H), 2.73 (h, $J = 6.9$ Hz, 1H), 2.18–2.12 (m, 2H), 1.29 (d, $J = 6.9$ Hz, 6H). ^{13}C NMR (150 MHz, CDCl_3): δ 175.1, 166.5, 159.3, 158.0, 145.6, 137.9, 130.6, 126.3, 122.2, 121.0, 120.7, 116.1, 110.7, 56.0, 35.5, 31.0, 26.8, 22.3, 19.0. HRMS (m/z): $[\text{M} + \text{H}]^+$ calcd for $\text{C}_{20}\text{H}_{21}\text{ClN}_4\text{O}_2\text{S}_2$, 449.0867; found, 449.0870.

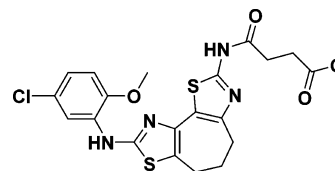


N-(8-((5-Chloro-2-methoxyphenyl)amino)-5,6-dihydro-4H-cyclohepta[1,2-d:3,4-d']bis(thiazole)-2-yl)-2-methylpentanamide (9d). The procedure for **9a** was followed, except 2-methylbutyryl chloride (8.54 μL , 0.069 mmol, 1.3 equiv) was substituted, yielding a yellow solid (11.8 mg, 48%). mp 138–144 $^\circ\text{C}$. IR (neat): ν_{max} 3207, 2031, 2011, 1969, 1531, 1261, 1178, 1090, 1016, 897, 798, 644 cm^{-1} . ^1H NMR (600 MHz, CDCl_3): δ 8.22 (s, 1H), 8.05 (d, $J = 2.4$ Hz, 1H), 7.57 (s, 1H), 6.92 (dd, $J = 8.6$, 2.5 Hz, 1H), 6.78 (d, $J = 8.7$ Hz, 1H), 3.90 (s, 3H), 3.05 (at, $J = 5.7$ Hz, 2H), 2.99 (at, $J = 5.6$ Hz, 2H), 2.52–2.46 (m, 1H), 2.17–2.13 (m, 2H), 1.84–1.76 (m, 1H), 1.61–

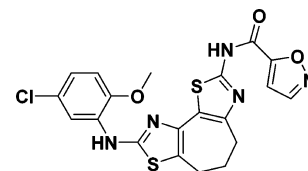
1.54 (m, 1H), 1.26 (d, $J = 7.0$ Hz, 3H), 0.96 (t, $J = 7.4$ Hz, 3H). ^{13}C NMR (150 MHz, CDCl_3): δ 175.1, 166.5, 159.3, 158.0, 145.6, 137.9, 130.6, 126.3, 122.2, 121.0, 120.8, 116.1, 110.7, 56.0, 38.7, 35.5, 32.3, 31.0, 26.8, 22.3, 19.0. HRMS (m/z): $[\text{M} + \text{H}]^+$ calcd for $\text{C}_{21}\text{H}_{23}\text{ClN}_4\text{O}_2\text{S}_2$, 463.1024; found, 463.1024.



Methyl 4-((8-((5-chloro-2-methoxyphenyl)amino)-5,6-dihydro-4H-cyclohepta[1,2-d:3,4-d']bis(thiazole)-2-yl)amino)-4-oxobutanoate (9e). The procedure for **9a** was followed, except 3-(carbomethoxy)-propionyl chloride (28.7 μL , 0.233 mmol, 2.2 equiv) was substituted, yielding a yellow solid (7.9 mg, 15%). ^1H NMR (600 MHz, CDCl_3): δ 8.07 (d, $J = 2.3$ Hz, 1H), 7.56 (s, 1H), 6.91 (dd, $J = 8.6$, 2.3 Hz, 1H), 6.77 (d, $J = 8.6$, 1H), 3.89 (s, 3H), 3.71 (s, 3H), 3.09 (at, $J = 5.5$ Hz, 2H), 2.98 (at, $J = 5.5$ Hz, 2H), 2.81–2.73 (m, 2H), 2.17–2.12 (m, 2H). ^{13}C NMR (150 MHz, CDCl_3): δ 173.1, 168.7, 159.0, 155.4, 145.7, 138.5, 130.8, 126.3, 123.1, 120.8, 120.2, 115.9, 113.1, 110.6, 56.0, 52.1, 32.6, 31.0, 28.9, 27.2, 22.6. HRMS (m/z): $[\text{M} + \text{H}]^+$ calcd for $\text{C}_{21}\text{H}_{21}\text{ClN}_4\text{O}_4\text{S}_2$, 493.0766; found, 493.0758.

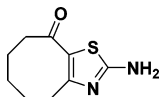


N-(8-((5-Chloro-2-methoxyphenyl)amino)-5,6-dihydro-4H-cyclohepta[1,2-d:3,4-d']bis(thiazole)-2-yl)isoxazole-5-carboxamide (9f). The procedure for **9a** was followed, except isoxazole 5-carboxyl chloride (6.64 μL , 0.069 mmol, 1.3 equiv) was substituted, yielding a bright yellow solid (11.7 mg, 47%). mp 115–120 $^\circ\text{C}$. IR (neat): ν_{max} 2924, 1597, 1531, 1415, 1294, 1244, 1124, 1020, 750 cm^{-1} . ^1H NMR (400 MHz, $\text{DMSO}-d_6$): δ 9.72 (s, 1H), 8.78 (d, $J = 2.0$ Hz, 1H), 8.61 (d, $J = 2.4$ Hz, 1H), 8.11 (s, 1H), 7.36 (s, 1H), 7.0 (d, $J = 8.7$ Hz, 1H), 6.96 (dd, $J = 8.6$, 2.5 Hz, 1H), 3.85 (s, 3H), 3.04 (at, $J = 5.6$ Hz, 2H), 2.94 (at, $J = 5.5$ Hz, 2H), 2.05–2.00 (m, 2H). HRMS (m/z): $[\text{M} + \text{H}]^+$ calcd $\text{C}_{20}\text{H}_{16}\text{ClN}_5\text{O}_3\text{S}_2$, 474.0456; found, 474.0462.

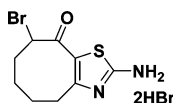


2-Amino-5,6,7,8-tetrahydrocycloocta[d]thiazol-9(4H)-one (A). To a heterogeneous mixture of cyclooctane-1,3-dione (2.08 g, 14.8 mmol) in $\text{CCl}_4/\text{water}$ (1:1, 50 mL) was added a solution of Br_2 (2.61 g, 0.84 mL, 16.3 mmol) in CCl_4 (25 mL) dropwise at 0 $^\circ\text{C}$. The mixture was stirred at 0 $^\circ\text{C}$ for 1 h and extracted with DCM. The organic layer was collected, and DCM was removed under reduced pressure to afford 2-bromocyclooctane-1,3-dione as a yellow oil which was used without further purification. To a solution of 2-bromocyclooctane-1,3-dione in anhydrous EtOH (35 mL) was added thiourea (1.24 g, 16.3 mmol). The mixture was stirred at room temperature overnight. EtOH was removed under reduced pressure, and the resulting light brown residue was redissolved in water (50 mL), basified with concentrated NH_4OH solution until pH = 8–9, and extracted with EtOAc (3×50 mL). The combined organics were dried over anhydrous Na_2SO_4 and concentrated to give the crude product which was triturated with CHCl_3 to afford **A** as a yellow solid (1.47 g, 51% yield over two steps). ^1H NMR (600 MHz, $\text{DMSO}-d_6$): δ 7.88 (s, 2H), 3.01 (t, $J = 7.0$ Hz, 2H), 2.78 (t, $J = 7.0$ Hz, 2H), 1.73–1.55 (m, 4H), 1.45–1.33 (m, 2H).

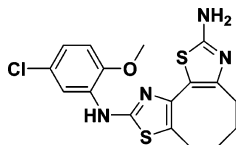
^{13}C NMR (150 MHz, $\text{DMSO}-d_6$): δ 191.1, 171.6, 159.9, 125.4, 39.6, 30.0, 24.0, 23.1, 22.6. HRMS (m/z): $[\text{M} + \text{H}]^+$ calcd $\text{C}_9\text{H}_{12}\text{N}_2\text{OS}$, 197.0749; found, 197.0749.



2-Amino-8-bromo-5,6,7,8-tetrahydrocycloocta[d]thiazol-9(4H)-one dihydrobromide salt (B). Compound A (0.70 g, 3.59 mmol) dissolved in glacial acetic acid (18 mL) was treated dropwise with a solution of HBr in HOAc (18 mL, 33 wt % in acetic acid). The mixture was stirred at room temperature for 30 min. Br_2 (0.573 g, 0.184 mL, 3.59 mmol) was added dropwise. The reaction mixture was stirred at room temperature for 1 h. Removing solvent under reduced pressure yielded the crude product which was triturated with DCM to afford **B** as a tan solid (1.08 g, 70%). ^1H NMR (600 MHz, $\text{DMSO}-d_6$): δ 10.26 (s, 1H), 9.35 (s, 3H), 5.84 (dd, J = 11.9, 7.2 Hz, 1H), 3.42–3.26 (m, 1H), 2.97 (dd, J = 15.1, 6.5 Hz, 1H), 2.23 (dtd, J = 13.5, 7.2, 3.3 Hz, 1H), 2.05 (t, J = 12.6 Hz, 1H), 1.75 (dd, J = 13.5, 6.5 Hz, 1H), 1.62 (dd, J = 9.7, 5.5 Hz, 2H), 1.42–1.24 (m, 1H). ^{13}C NMR (150 MHz, $\text{DMSO}-d_6$): δ 184.5, 170.0, 150.0, 121.0, 55.7, 35.6, 27.1, 23.5, 22.4. HRMS (m/z): $[\text{M} + \text{H}]^+$ calcd for $\text{C}_9\text{H}_{11}\text{BrN}_2\text{OS}$, 274.9854; found, 274.9867.

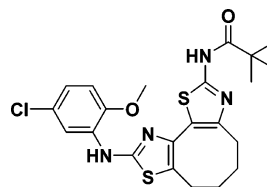


N-9-((5-Chloro-2-methoxyphenyl)amino)-4,5,6,7-tetrahydrocycloocta[1,2-d:3,4-d']bis(thiazole)-2,9-diamine (8a). A suspension of **B** (0.451 g, 1.03 mmol, 1.0 equiv) and 1-((5-chloro-2-methoxyphenyl)thiourea) (0.224 g, 1.03 mmol, 1.0 equiv) in anhydrous EtOH (10 mL) was heated at reflux for 24 h. EtOH was removed under reduced pressure, and the residue was redissolved in water (10 mL), basified with 1 M NaOH (50 mL), and extracted with EtOAc (2 \times 50 mL). The combined organics were dried over anhydrous Na_2SO_4 , concentrated, and purified by column chromatography (100% EtOAc, R_f = 0.20) to afford **8a** as a light brown solid (0.266 g, 65%). ^1H NMR (600 MHz, CDCl_3): δ 8.05 (d, J = 2.3 Hz, 1H), 7.67 (s, 1H), 6.88 (dd, J = 8.6, 2.3 Hz, 1H), 6.75 (d, J = 8.6 Hz, 1H), 6.12 (s, 2H), 3.85 (s, 3H), 2.79 (t, J = 10.5 Hz, 4H), 1.78 (dt, J = 10.5, 5.2 Hz, 4H). ^{13}C NMR (150 MHz, CDCl_3): δ 167.3, 159.5, 145.8, 138.8, 130.9, 126.2, 123.2, 121.9, 121.0, 116.3, 115.4, 110.8, 56.1, 29.5, 27.3, 24.5, 23.5. HRMS (m/z): $[\text{M} + \text{H}]^+$ calcd for $\text{C}_{17}\text{H}_{17}\text{ClN}_4\text{OS}_2$, 393.0611; found, 393.0593.

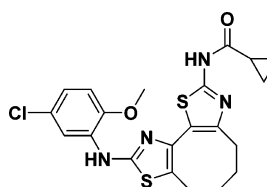


N-9-((5-Chloro-2-methoxyphenyl)amino)-4,5,6,7-tetrahydrocycloocta[1,2-d:3,4-d']bis(thiazole)-2-yl)pivalamide (10a). To a solution of **8a** (0.266 g, 0.676 mmol, 1.0 equiv) in anhydrous DCM (7 mL) was added TEA (188 μL , 1.35 mmol, 2.0 equiv). Pivaloyl chloride (92 μL , 0.743 mmol, 1.1 equiv) was then added in one portion. The reaction mixture was purged with nitrogen and stirred at 60 $^\circ\text{C}$ overnight at which time LC-MS indicated the completion of reaction. DCM was removed in vacuo, and the resulting solid was purified by HPLC to yield **10a** as a yellow solid (0.183 g, 57%). ^1H NMR (600 MHz, CDCl_3): δ 9.46 (s, 1H), 8.07 (d, J = 2.5 Hz, 1H), 7.64 (s, 1H), 6.97–6.84 (m, 1H), 6.77 (dd, J = 8.6, 2.5 Hz, 1H), 3.88 (d, J = 3.0 Hz, 3H), 2.93–2.77 (m, 4H), 1.81 (m, 4H), 1.34 (s, 9H). ^{13}C NMR (150 MHz, CDCl_3): δ 175.8, 159.4, 157.3, 146.6, 145.7, 139.0, 130.8, 126.3, 122.8, 120.9, 120.9, 116.1, 110.7, 56.1, 39.2, 29.9, 27.3, 27.0, 24.7, 24.3. HRMS (m/z): $[\text{M} + \text{H}]^+$ calcd for $\text{C}_{22}\text{H}_{25}\text{ClN}_4\text{O}_2\text{S}_2$, 477.1186; found, 477.1176.

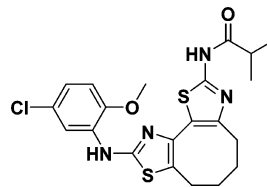
N-9-((5-Chloro-2-methoxyphenyl)amino)-4,5,6,7-tetrahydrocycloocta[1,2-d:3,4-d']bis(thiazole)-2-yl)-



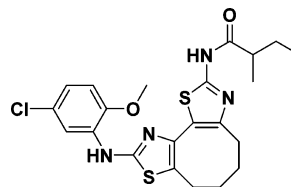
cyclopropanecarboxamide (10b). The procedure for **10a** was followed, except cyclopropane carbonyl chloride (83 μL , 0.917 mmol, 1.1 equiv) was substituted, yielding a yellow solid (0.0359 g, 9%). ^1H NMR (600 MHz, CDCl_3): δ 11.15 (s, 1H), 8.04 (d, J = 2.2 Hz, 1H), 7.80 (s, 1H), 6.89 (dt, J = 8.6, 2.2 Hz, 1H), 6.75 (dd, J = 8.6, 2.2 Hz, 1H), 3.85 (d, J = 3.4 Hz, 3H), 2.90–2.77 (m, 4H), 1.78 (s, 4H), 1.61 (tt, J = 8.1, 4.6 Hz, 1H), 1.20–1.15 (m, 2H), 0.90 (dt, J = 7.2, 3.4 Hz, 2H). ^{13}C NMR (150 MHz, CDCl_3): δ 171.8, 159.7, 158.4, 146.7, 146.0, 139.0, 130.9, 126.2, 122.6, 121.2, 120.6, 116.4, 110.8, 56.1, 29.9, 27.1, 24.8, 24.4, 15.0, 9.2. HRMS (m/z): $[\text{M} + \text{H}]^+$ calcd for $\text{C}_{21}\text{H}_{21}\text{ClN}_4\text{O}_2\text{S}_2$, 461.0873; found, 461.0865.



N-9-((5-Chloro-2-methoxyphenyl)amino)-4,5,6,7-tetrahydrocycloocta[1,2-d:3,4-d']bis(thiazole)-2-yl)isobutyramide (10c). The procedure for **10a** was followed, except isobutyryl chloride (87 μL , 0.830 mmol, 1.2 equiv) was substituted, yielding a yellow solid (0.132 g, 41%). ^1H NMR (600 MHz, CDCl_3): δ 9.56 (s, 1H), 8.04 (d, J = 2.5 Hz, 1H), 7.81 (s, 1H), 6.94–6.83 (m, 1H), 6.75 (d, J = 8.6 Hz, 1H), 3.84 (s, 3H), 2.90–2.78 (m, 4H), 2.59 (hept, J = 6.9 Hz, 1H), 1.84–1.74 (m, 4H), 1.23 (d, J = 6.9 Hz, 6H). ^{13}C NMR (150 MHz, CDCl_3): δ 174.5, 159.7, 157.6, 146.9, 145.9, 139.0, 130.9, 126.2, 122.6, 121.1, 120.8, 116.4, 110.8, 56.1, 35.6, 30.0, 27.1, 24.7, 24.4, 19.3. HRMS (m/z): $[\text{M} + \text{H}]^+$ calcd for $\text{C}_{21}\text{H}_{23}\text{ClN}_4\text{O}_2\text{S}_2$, 463.1029; found, 463.1021.

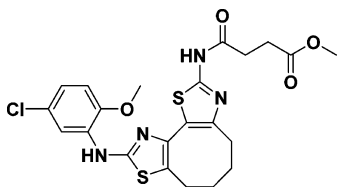


N-9-((5-Chloro-2-methoxyphenyl)amino)-4,5,6,7-tetrahydrocycloocta[1,2-d:3,4-d']bis(thiazole)-2-yl)-2-methylbutanamide (10d). The procedure for **10a** was followed, except 2-methylbutyryl chloride (85 μL , 0.683 mmol, 1.1 equiv) was substituted, yielding a light yellow solid (0.10 g, 34%). ^1H NMR (600 MHz, CDCl_3): δ 9.72 (s, 1H), 8.02 (d, J = 2.4 Hz, 1H), 7.85 (s, 1H), 6.88 (dd, J = 8.6, 2.4 Hz, 1H), 6.75 (d, J = 8.6 Hz, 1H), 3.84 (s, 3H), 3.04–2.61 (m, 4H), 2.35 (sextet, J = 7.0 Hz, 1H), 1.89–1.66 (m, 5H), 1.50 (dp, J = 14.0, 7.0 Hz, 1H), 1.20 (d, J = 7.0 Hz, 3H), 0.89 (t, J = 7.0 Hz, 3H). ^{13}C NMR (150 MHz, CDCl_3): δ 174.1, 159.7, 157.5, 146.9, 146.0, 139.0, 130.9, 126.2, 122.6, 121.2, 120.8, 116.4, 110.8, 56.1, 42.8, 30.0, 27.2, 27.1, 24.7, 24.3, 17.1, 11.8. HRMS (m/z): $[\text{M} + \text{H}]^+$ calcd for $\text{C}_{22}\text{H}_{25}\text{ClN}_4\text{O}_2\text{S}_2$, 477.1186; found, 477.1176.

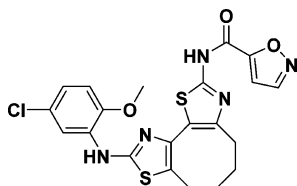


Methyl 4-((9-((5-chloro-2-methoxyphenyl)amino)-4,5,6,7-tetrahydrocycloocta[1,2-d:3,4-d']bis(thiazole)-2-yl)amino)-4-oxo-

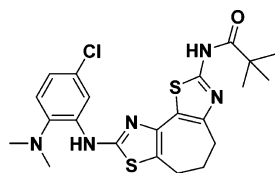
butanoate (**10e**). The procedure for **10a** was followed, except methyl 4-chloro-4-oxobutylate (76 μ L, 0.618 mmol, 1.1 equiv) was substituted, yielding a light yellow solid (0.121 g, 42%). ^1H NMR (600 MHz, CDCl_3): δ 10.63 (s, 1H), 8.05 (d, $J = 2.5$ Hz, 1H), 7.91 (s, 1H), 6.85 (dd, $J = 8.6, 2.5$ Hz, 1H), 6.72 (d, $J = 8.6$ Hz, 1H), 3.80 (s, 3H), 3.65 (s, 3H), 2.85 (d, $J = 7.0$ Hz, 2H), 2.80–2.72 (m, 6H), 1.80–1.70 (m, 4H). ^{13}C NMR (150 MHz, CDCl_3): δ 173.1, 169.5, 159.7, 157.4, 147.1, 145.9, 138.9, 130.8, 126.0, 122.4, 121.0, 120.6, 116.4, 110.7, 56.0, 52.0, 30.7, 29.9, 28.7, 27.0, 24.5, 24.2. HRMS (m/z): $[\text{M} + \text{H}]^+$ calcd for $\text{C}_{22}\text{H}_{23}\text{ClN}_4\text{O}_4\text{S}_2$, 507.0927; found, 507.0918.



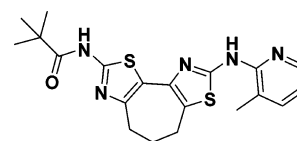
N-(9-((5-Chloro-2-methoxyphenyl)amino)-4,5,6,7-tetrahydrocyclo-octa[1,2-d:3,4-d']bis(thiazole)-2-yl)isoxazole-5-carboxamide (**10f**). The procedure for **10a** was followed, except isoxazole-5-carbonyl chloride (76 μ L, 0.787 mmol, 1.1 equiv) was substituted, yielding a yellow solid (0.0422 g, 12%). ^1H NMR (600 MHz, CDCl_3): δ 9.55 (s, 1H), 8.39 (d, $J = 1.7$ Hz, 1H), 8.07 (d, $J = 2.4$ Hz, 1H), 7.76 (s, 1H), 7.15–7.11 (m, 1H), 6.90 (dd, $J = 8.6, 2.4$ Hz, 1H), 6.77 (d, $J = 8.6$ Hz, 1H), 3.87 (s, 3H), 2.97–2.75 (m, 4H), 1.88–1.75 (m, 4H). ^{13}C NMR (150 MHz, CDCl_3): δ 161.6, 159.8, 156.9, 153.7, 151.3, 146.4, 145.9, 138.5, 130.8, 126.3, 123.0, 121.9, 121.2, 116.3, 110.9, 108.3, 56.1, 29.7, 27.0, 24.6, 24.0. HRMS (m/z): $[\text{M} + \text{H}]^+$ calcd for $\text{C}_{21}\text{H}_{18}\text{ClN}_5\text{O}_3\text{S}_2$, 488.0618; found, 488.0609.



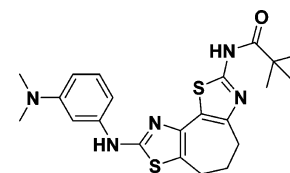
N-(8-((5-Chloro-2-(dimethylamino)phenyl)amino)-5,6-dihydro-4H-cyclohepta[1,2-d:3,4-d']bis(thiazole)-2-yl)pivalamide (**9g**). The procedures for **7a** and **9a** were followed, except 1-(5-chloro-2-(dimethylamino)-phenyl)thiourea (0.229 g, 1.1 mmol, 1.1 equiv) was substituted, yielding a yellow solid (0.015 g, 15%). ^1H NMR (400 MHz, CDCl_3): δ 8.28 (s, 1H), 7.99 (d, $J = 2.3$, 1H), 7.07 (d, $J = 8.4$, 1H), 6.91 (dd, $J = 2.3, 8.4$, 1H), 3.18–2.85 (m, 4H), 2.64 (s, 6H), 2.15 (s, 2H), 1.35 (s, 9H). ^{13}C NMR (100 MHz, CDCl_3): δ 184.3, 176.2, 159.2, 156.9, 145.3, 140.2, 138.8, 136.7, 130.8, 122.8, 121.4, 120.7, 115.6, 44.9, 39.3, 38.7, 32.3, 27.5, 22.8. HRMS (m/z): $[\text{M} + \text{H}]^+$ calcd for $\text{C}_{22}\text{H}_{27}\text{ClN}_5\text{OS}_2$, 476.1340; found, 476.1338.



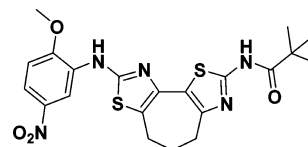
N-(8-((3-Methylpyridin-2-yl)amino)-5,6-dihydro-4H-cyclohepta[1,2-d:3,4-d']bis(thiazole)-2-yl)pivalamide (**10h**). The procedures for **7a** and **9a** were followed, except 1-(3-methylpyridin-2-yl)thiourea (0.167 g, 1.1 mmol, 1.1 equiv) was substituted, yielding a yellow solid (0.024 g, 26%). mp 154–155 $^{\circ}\text{C}$. ^1H NMR (400 MHz, CDCl_3): δ 8.85 (br s, 1H), 8.16 (d, $J = 4.0$, 1H), 7.97 (br s, 1H), 7.37 (d, $J = 7.1$, 1H), 6.78 (dd, $J = 5.1, 7.2$, 1H), 3.13–2.93 (m, 4H), 2.27 (s, 3H), 2.14–2.10 (m, 2H), 1.30 (s, 9H). ^{13}C NMR (100 MHz, CDCl_3): δ 175.6, 156.5, 155.2, 149.7, 145.9, 144.4, 138.3, 137.0, 123.5, 123.3, 117.8, 116.5, 39.3, 33.1, 27.5, 27.0, 23.0, 16.8. HRMS (m/z): $[\text{M} + \text{H}]^+$ calcd for $\text{C}_{20}\text{H}_{23}\text{N}_5\text{OS}_2$, 414.1417; found, 414.1404.



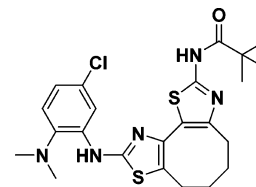
N-(8-((3-(Dimethylamino)phenyl)amino)-5,6-dihydro-4H-cyclohepta[1,2-d:3,4-d']bis(thiazole)-2-yl)pivalamide (**10i**). The procedures for **7a** and **9a** were followed, except 1-(2-(dimethylamino)-phenyl)thiourea (0.195 g, 1.1 mmol, 1.1 equiv) was substituted, yielding a yellow solid (0.010g, 10%). mp 111–112 $^{\circ}\text{C}$. ^1H NMR (600 MHz, CDCl_3): δ 9.09 (s, 1H), 7.21 (s, 1H), 7.18 (t, $J = 8.2$ Hz, 1H), 7.00 (s, 1H), 6.59 (d, $J = 8.2$, 1H), 6.45 (d, $J = 8.2$, 1H), 3.07 (t, $J = 5.7$ Hz, 2H), 3.01 (s, 3H), 2.95 (t, $J = 5.7$ Hz, 2H), 2.16–2.12 (m, 2H), 1.32 (s, 9H). ^{13}C NMR (150 MHz, CDCl_3): δ 175.8, 161.1, 155.8, 151.6, 145.3, 141.5, 138.4, 130.0, 123.3, 119.5, 107.5, 106.5, 102.5, 40.9, 39.3, 32.6, 29.9, 27.5, 22.9. HRMS (m/z): $[\text{M} + \text{H}]^+$ calcd for $\text{C}_{22}\text{H}_{27}\text{N}_5\text{OS}_2$, 442.1730; found, 442.1725.



N-(8-((2-Methoxy-5-nitrophenyl)amino)-5,6-dihydro-4H-cyclohepta[1,2-d:3,4-d']bis(thiazole)-2-yl)pivalamide (**10j**). The procedures for **7a** and **9a** were followed, except 1-(2-methoxy-5-nitrophenyl)thiourea (0.227 g, 1.1 mmol, 1.1 equiv) was substituted, yielding a yellow solid (0.006 g, 6%). ^1H NMR (600 MHz, CDCl_3): δ 10.60 (s, 1H), 8.89 (s, 1H), 7.94 (d, $J = 9.3$, 1H), 7.62 (s, 1H), 6.94 (d, $J = 9.3$, 1H), 3.97 (s, 3H), 3.13–2.94 (m, 4H), 2.25–2.05 (m, 2H), 1.25 (s, 9H). ^{13}C NMR (150 MHz, DMSO): δ 176.1, 159.1, 155.7, 152.4, 146.2, 140.8, 137.5, 130.4, 121.1, 120.5, 117.4, 111.1, 110.1, 56.6, 38.7, 32.3, 26.7, 26.1, 22.3. HRMS (m/z): $[\text{M} + \text{H}]^+$ calcd for $\text{C}_{21}\text{H}_{23}\text{N}_5\text{O}_4\text{S}_2$, 474.1264; found, 474.1253.

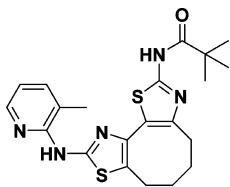


N-(9-((5-Chloro-2-(dimethylamino)phenyl)amino)-4,5,6,7-tetrahydrocyclo-octa[1,2-d:3,4-d']bis(thiazole)-2-yl)pivalamide (**10g**). The procedures for **8a** and **10a** was followed, except 1-(5-chloro-2-(dimethylamino)-phenyl)thiourea (0.260 g, 1.13 mmol, 1.0 equiv) was substituted, yielding a tan solid (0.146 g, 53%). ^1H NMR (600 MHz, CDCl_3): δ 8.92 (s, 1H), 8.37 (s, 1H), 8.02 (d, $J = 2.3$ Hz, 1H), 7.02 (d, $J = 8.4$ Hz, 1H), 6.84 (dd, $J = 8.4, 2.3$ Hz, 1H), 2.87–2.72 (m, 4H), 2.56 (s, 6H), 1.82–1.67 (m, 4H), 1.27 (s, 9H). ^{13}C NMR (150 MHz, CDCl_3): δ 175.6, 159.3, 156.9, 147.3, 140.0, 139.1, 136.5, 130.4, 122.4, 121.2, 121.1, 120.8, 115.6, 44.7, 39.0, 30.0, 27.2, 26.8, 24.7, 24.3. HRMS (m/z): $[\text{M} + \text{H}]^+$ calcd for $\text{C}_{23}\text{H}_{28}\text{ClN}_5\text{OS}$, 490.1502; found, 490.1491.

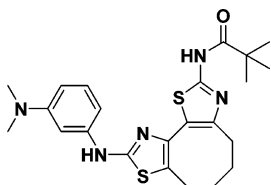


N-(9-((3-Methylpyridin-2-yl)amino)-4,5,6,7-tetrahydrocyclo-octa[1,2-d:3,4-d']bis(thiazole)-2-yl)pivalamide (**10h**). The procedure for **8a** and **10a** was followed, except 1-(3-methylpyridin-2-yl)thiourea (0.171 g, 1.02 mmol, 1.0 equiv) was substituted, yielding a yellow solid (0.0845 g, 40%). ^1H NMR (600 MHz, CDCl_3): δ 8.97 (s, 1H), 8.45–7.82 (m, 2H), 7.35 (d, $J = 7.2$ Hz, 1H), 6.92–6.59 (m, 1H), 2.81 (s,

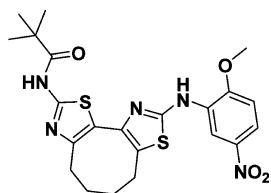
4H), 2.21 (s, 3H), 1.76 (s, 4H), 1.26 (s, 9H). ^{13}C NMR (150 MHz, CDCl_3): δ 175.5, 156.7, 156.6, 149.6, 147.1, 144.1, 138.1, 137.1, 125.3, 120.9, 117.7, 116.3, 39.0, 30.1, 27.3, 27.2, 24.4, 24.3, 16.7. HRMS (m/z): $[\text{M} + \text{H}]^+$ calcd for $\text{C}_{21}\text{H}_{25}\text{N}_5\text{OS}_2$, 428.1579; found, 428.1570.



N-(9-((3-(Dimethylamino)phenyl)amino)-4,5,6,7-tetrahydrocycloocta[1,2-d:3,4-d']bis(thiazole)-2-yl)pivalamide (**10i**). The procedure for **8a** and **10a** was followed, except 1-(3-(dimethylamino)phenyl)thiourea (0.197 g, 1.01 mmol, 1.0 equiv) was substituted, yielding a tan solid (0.0817 g, 22%). ^1H NMR (600 MHz, CDCl_3): δ 8.92 (s, 1H), 8.26 (s, 1H), 7.12 (t, $J = 8.1$ Hz, 1H), 6.77 (t, $J = 2.1$ Hz, 1H), 6.60 (dd, $J = 7.8, 1.9$ Hz, 1H), 6.39 (d, $J = 8.3$ Hz, 1H), 2.92 (s, 6H), 2.90–2.67 (m, 4H), 1.88–1.69 (m, 4H), 1.26 (s, 9H). ^{13}C NMR (150 MHz, CDCl_3): δ 175.6, 161.8, 157.0, 151.5, 146.9, 141.5, 138.5, 129.8, 121.2, 121.1, 107.2, 106.5, 102.4, 40.6, 39.0, 30.0, 27.2, 26.8, 24.7, 24.5. HRMS (m/z): $[\text{M} + \text{H}]^+$ calcd for $\text{C}_{23}\text{H}_{29}\text{N}_5\text{OS}_2$, 456.1892; found, 456.1884.



N-(9-((2-Methoxy-5-nitrophenyl)amino)-4,5,6,7-tetrahydrocycloocta[1,2-d:3,4-d']bis(thiazole)-2-yl)pivalamide (**10j**). The procedure for **8a** and **10a** was followed, except 1-(2-methoxy-5-nitrophenyl)thiourea (0.229 g, 1.01 mmol, 1.0 equiv) was substituted, yielding a yellow solid (0.0997 g, 34%). ^1H NMR (600 MHz, CDCl_3): δ 9.04 (d, $J = 2.7$ Hz, 1H), 8.90 (s, 1H), 7.77 (dd, $J = 9.0, 2.7$ Hz, 2H), 6.84 (d, $J = 9.0$ Hz, 1H), 3.94 (s, 3H), 2.90–2.72 (m, 4H), 1.86–1.67 (m, 4H), 1.28 (s, 9H). ^{13}C NMR (150 MHz, CDCl_3): δ 175.6, 158.6, 157.0, 151.5, 147.2, 141.7, 139.2, 130.1, 122.9, 120.8, 117.6, 110.9, 108.9, 56.5, 39.1, 29.9, 27.2, 26.8, 24.6, 24.3. HRMS (m/z): $[\text{M} + \text{H}]^+$ calcd for $\text{C}_{22}\text{H}_{25}\text{N}_5\text{O}_4\text{S}_2$, 488.1426; found, 488.1415.



■ ASSOCIATED CONTENT

Supporting Information

^1H and ^{13}C NMR spectra as well as a corrector activity figure for compounds **9a**, **10a**, **9e**, and **10c**; HRMS data summary for all compounds; and computational data. This material is available free of charge via the Internet at <http://pubs.acs.org>.

■ AUTHOR INFORMATION

Corresponding Author

*E-mail: mjkurth@ucdavis.edu. Fax: (530) 752-8995. Tel.: (530) 554-2145.

Notes

The authors declare no competing financial interest.

■ ACKNOWLEDGMENTS

We thank Professor Makhlu J. Haddadin (American University of Beirut, Beirut, Lebanon) for helpful insights and Kelli Gottlieb for assistance collecting HRMS data. The authors thank the Tara K. Telford Fund for Cystic Fibrosis Research at UC Davis, the National Institutes of Health (DK072517 and GM076151), the National Science Foundation (CHE-0614756, CHE-0443516, CHE-0449845, CHE-9808183 – NMR spectrometers; CHE-030089—computer time from the Pittsburgh Supercomputer Center), and the Petroleum Research Fund of the American Chemical Society (grant 52801-ND4) for their generous support. This work used the Extreme Science and Engineering Discovery Environment (XSEDE), which is supported by the National Science Foundation [ACI-1053575].

■ ABBREVIATIONS:

cystic fibrosis transmembrane conductance regulator, (CFTR); cystic fibrosis, (CF); Fischer rat thyroid, (FRT); yellow fluorescent protein, (YFP); electron-withdrawing group, (EWG); electron-donating group, (EDG)

■ REFERENCES

- (1) Bobadilla, J. L.; Macek, M., Jr.; Fine, J. P.; Farrell, P. M. Cystic fibrosis: a worldwide analysis of CFTR mutations — correlation with incidence data and application to screening. *Hum. Mutat.* **2002**, *19*, 575–606.
- (2) CF mutation database: genet.sickkids.on.ca/cftr/StatisticsPage.html (accessed 5/2/2014).
- (3) Cystic Fibrosis Foundation Patient Registry 2012 Annual Data Report: <http://www.cff.org/livingwithcf/qualityimprovement/patientregistryreport/> (accessed 5/2/2014).
- (4) (a) Amaral, M. D.; Kunzelmann, K. Molecular targeting of CFTR as a therapeutic approach to cystic fibrosis. *Trends Pharmacol. Sci.* **2007**, *28*, 334–341. (b) Amaral, M. D. CFTR and chaperones: processing and degradation. *J. Mol. Neurosci.* **2004**, *23*, 41–48. (c) Amaral, M. D. Therapy through chaperones: sense or anti-sense? Cystic fibrosis as a model disease. *J. Inherit. Metab. Dis.* **2005**, *29*, 477–487.
- (5) (a) Pedemonte, N.; Lukacs, G. L.; Du, K.; Caci, E.; Zegarar-Moran, O.; Galletta, L. J. V.; Verkman, A. S. Small-molecule correctors of defective Delta F508-CFTR cellular processing identified by high-throughput screening. *J. Clin. Invest.* **2005**, *115*, 2564–2571. (b) Verkman, A. S.; Galletta, L. J. Chloride Channels as Drug Targets. *Nat. Rev. Drug Discovery* **2009**, *8*, 153–171. (c) Lukacs, G. L.; Verkman, A. S. CFTR: Folding, Misfolding and Correcting the DeltaF508 Conformational Defect. *Trends Mol. Med.* **2012**, *18*, 81–91. (d) Okiyoneda, T.; Veit, G.; Dekkers, J. F.; Bagdany, M.; Soya, N.; Xu, H.; Roldan, A.; Verkman, A. S.; Kurth, M.; Simon, A.; Hegedus, T.; Beekman, J. M.; Lukacs, G. L. Mechanism-based corrector combination restores DeltaF508-CFTR folding and function. *Nat. Chem. Biol.* **2013**, *9*, 444–454.
- (6) (a) Wang, Y.; Wrennall, J. A.; Cai, Z.; Li, H.; Sheppard, D. N. Understanding how cystic fibrosis mutations disrupt CFTR function: From single molecules to animal models. *Int. J. Biochem. Cell B* **2014**, *52*, 47–57. (b) Ramsey, B. W.; Davies, J.; McElvaney, N. G.; Tullis, E.; Bell, S. C.; Dřevínek, P.; Griese, M.; McKone, E. F.; Wainwright, C. E.; Konstan, M. W.; Moss, R.; Ratjen, F.; Sermet-Gaudelus, I.; Rowe, S. M.; Dong, Q.; Rodriguez, S.; Yen, K.; Ordoñez, C.; Elborn, J. S. A CFTR potentiator in patients with cystic fibrosis and the G551D mutation. *N. Engl. J. Med.* **2011**, *365*, 1663–1672. (c) Van Goor, F.; Yu, H.; Burton, B.; Hoffman, B. J. Effect of ivacaftor on CFTR forms with missense mutations associated with defects in protein processing or function. *J. Cyst. Fibros.* **2014**, *13*, 29–36.
- (7) (a) Deeks, E. D. Ivacaftor: A Review of Its Use in Patients with Cystic Fibrosis. *Drugs* **2013**, *73*, 1595. (b) Kopeikin, Z.; Yuksek, Z.; Yang, H.-Y.; Bompadre, S. G. Combined effects of VX-770 and VX-

809 on several functional abnormalities of F508del-CFTR channels. *J. Cystic Fibrosis* **2014**, DOI: 10.1016/j.jcf.2014.04.003.

(8) Yu, G. J.; Yoo, C. L.; Yang, B.; Lodewyk, M. W.; Meng, L.; El-Idreesy, T. T.; Fetting, J. C.; Tantillo, D. J.; Verkman, A. S.; Kurth, M. J. Potent *s*-cis-Locked Bithiazole Correctors of Δ F508 Cystic Fibrosis Transmembrane Conductance Regulator Cellular Processing for Cystic Fibrosis Therapy. *J. Med. Chem.* **2008**, *51*, 6044–6054.

(9) Vistoli, G.; Pedretti, A.; Testa, B. Assessing drug-likeness-what are we missing? *Drug Discovery Today* **2008**, *13*, 285–294.

(10) Du, L.; Chen, M.; Zhang, Y.; Shen, B. BlmIII and BlmIV Nonribosomal Peptide Synthetase-Catalyzed Biosynthesis of the Bleomycin Bithiazole Moiety Involving Both in *Cis* and in *Trans* Aminoacylation. *Biochemistry* **2003**, *42*, 9731–9740.

(11) Dinner, A. R.; Sali, A.; Smith, L. J.; Dobson, C. M.; Karplus, M. Understanding protein folding via free-energy surfaces from theory and experiment. *Trends Biochem. Sci.* **2000**, *25*, 331–339.

(12) Yoo, C. L.; Yu, G. J.; Yang, B.; Robins, L. I.; Verkman, A. S.; Kurth, M. J. 4'-Methyl-4,5'-bithiazole-based correctors of defective Δ F508-CFTR cellular processing. *Bioorg. Med. Chem. Lett.* **2008**, *18*, 2610–2614.

(13) Pirrung, M. C.; Webster, N. J. G. Mechanism of Intramolecular Photocycloadditions of Cyclooctenones. *J. Org. Chem.* **1987**, *52*, 3603–3613.

(14) Frisch, M. J.; et al. *Gaussian 09*, revision B.01; Gaussian, Inc., Wallingford, CT, 2009 (full reference in Supporting Information).

(15) Shao, Y.; et al. *Phys. Chem. Chem. Phys.* **2006**, *8*, 3172–3191 (full reference in Supporting Information).

(16) (a) Becke, A. D. Density-functional thermochemistry. III. The role of exact exchange. *J. Chem. Phys.* **1993**, *98*, 5648–5652. (b) Becke, A. D. A new mixing of Hartree–Fock and local-density-functional theories. *J. Chem. Phys.* **1993**, *98*, 1372–1377. (c) Lee, C.; Yang, W.; Parr, R. G. Development of the Colle–Salvetti correlation-energy formula into a functional of the electron density. *Phys. Rev. B* **1988**, *37*, 785–789. (d) Stephens, P. J.; Devlin, F. J.; Chabalowski, C. F.; Frisch, M. J. Ab initio calculation of vibrational absorption and circular dichroism spectra using density functional force fields. *J. Phys. Chem.* **1994**, *98*, 11623–11627.

(17) (a) Zhao, Y.; Truhlar, D. G. The M06 suite of density functionals for main group thermochemistry, thermochemical kinetics, noncovalent interactions, excited states, and transition elements: two new functionals and systematic testing of four M06-class functionals and 12 other functionals. *Theor. Chem. Acc.* **2008**, *120*, 215–241. (b) Zhao, Y.; Truhlar, D. G. Density Functionals with Broad Applicability in Chemistry. *Acc. Chem. Res.* **2008**, *41*, 157–167.

(18) CYLview, 1.0b; Legault, C. Y. Université de Sherbrooke, 2009 (<http://www.cylview.org>).